0273-2289/99/80/0039/$13.00

A Simple Structured Model for Continuous Production of a Hybrid Antibiotic by *Streptomyces lividans* Pellets in a Fluidized-Bed Bioreactor

Montserrat Sarrà,*[,1] Carlos Casas,[1] Manel Poch,[2] and Francesc Gòdia[1]

[1]Departament d'Enginyeria Química, Universitat Autònoma de Barcelona, Bellaterra, 08193 Barcelona, Spain, E-mail: Sarra@uab-eq.uab.es; and [2]Laboratori d'Enginyeria Química i Ambiental, Universitat de Girona, 17071 Girona, Spain

Received January 7, 1998; Accepted September 11, 1998

Abstract

A simple structured model is developed for the description of the experiments of continuous production of a hybrid antibiotic by *Streptomyces lividans* TK21 pellets in a fluidized-bed reactor. The model is based on the effect of internal and external phosphate concentrations on antibiotic production during cyclic feeding. These concentrations can be calculated on the basis of the equations postulated by the model. The model also considers the cell growth, reflected in changes of the pellet size along the culture. The model parameters are evaluated sequentially by performing experiments at different operational conditions. The validity of the model and its corresponding parameters is corroborated further by the satisfactory modeling of the bioreactor operation during an extended period of time at various operation conditions.

Index Entries: Hybrid antibiotic; continuous cultivation; fluidized-bed; mathematical model; immobilized cells; *Streptomyces*.

Introduction

Modeling of bioprocesses is a specialized topic concerned with a mathematical description of metabolic processes of the microorganisms that are contained in a bioreactor. Growth and secondary metabolite production from filamentous microorganisms are associated with complex

*Author to whom all correspondence and reprint requests should be addressed.

and poorly understood processes. In submerged cultures, the morphology of these microorganisms varies from free hyphae to large compact aggregates known as pellets, depending mainly on the culture conditions. The qualitative and quantitative measurement and control of the morphology is important because it determines the viscosity of the fermentation broth, and, in many cases, the productivity of secondary metabolites correlates with morphology. For example, the production of nikkomycin has been shown to be dependent on the pellet size of *Streptomyces tendae (1)* whereas penicillin production by *Penicillium chrysogenum* seems to require more filamentous growth *(2)*.

Mycelium is multicellular in structure and its morphology is very heterogeneous. This means that physiology and differentiation of cells change along the length of the hyphae and during fermentation. As a result, the complexity involved with both growth and metabolic production in filamentous microorganism, explains the fact that only a few structured models are available. The early work of Megee et al. *(3)* considers hyphal growth and differentiation and assumes different activities and metabolite synthesis of the differentiation states. Later, a combination of a morphological and an intracellularly structured model to predict the synthesis of cephalosporin C, an antibiotic produced by the filamentous fungus *Cephalosporium acremonium*, was proposed by Matsumura et al. *(4)*. Chu and Constantinides *(5)* proposed a model based on the model of Matsumura; Nestaas and Wang *(6)* described a simple morphologically structured model for penicillin production; Meyerhoff and Bellgardt *(7)* described *P. chrysogenum* fed-batch fermentation with a morphology-based model. Several models can explain the morphological development of mycelia *(8,10)*. A number of mathematical models based on a multienzymatic reaction system for the antibiotic production are also described in the literature *(11,12)*. Thomas et al. *(13)* and Paul and Thomas *(14)* reported a structured kinetic model describing growth, differentiation, and penicillin production in submerged *P. chrysogenum* cultures. In that model the antibiotic production is related to the proportion of the nongrowing regions of the hyphae, but still nondegenerated and nonlysed. Recently, King *(15)* described the growth of *S. tendae* and the production of nikkomycin by a highly structured model without any description of morphology. Although the model for cell growth can be extended to different strains, the antibiotic production follows different patterns, and therefore, the model cannot be applied in general *(16)*.

Secondary metabolism often occurs in a narrow range of specific growth rates or even at zero growth. Consequently, batch fermentations for products such as antibiotics often follow a biphasic pattern. Nevertheless, most of the models proposed consider only the batch cultivation and a few of them are extended to fed-batch operation. As a result, few attempts have been made to propose models for cell growth and secondary metabolite production in an immobilized live cell bioreactor. The continuous produc-

tion of candicidin by *Streptomyces griseus* could be improved by modeling and simulating the cycle pulsing of the growth-limiting nutrient *(17)*.

The objective of this work is to propose a simple structured model for the continuous production of a hybrid antibiotic by immobilized cells of a transformed strain of *Streptomyces lividans* TK21. The clone contains the plasmid pMH 9410, which has a chromosomal DNA fragment from *Streptomyces antibioticus* ATCC11891 and produces a diffusible pigmented antibiotic. This is an isochromanequinone antibiotic and has inhibitory activity against various bacterial species, such as *Bacillus subtilis* and *Vibrio alginolyticus*. The need for postulating a structured model clearly derives from the dependence of antibiotic production on the internal phosphate storage as well as on the external phosphate concentration. In summary, mathematical modeling can be a helpful tool for understanding, controlling, and optimizing antibiotic productivity.

Materials and Methods

Microorganism and Culture Conditions

The transformed strain of *S. lividans* TK21 used in this study was kindly given by Dr. F. Malpartida (Centro Nacional de Biotecnologia, Madrid).

Cultivations were carried out in a three-phase fluidized-bed bioreactor, with a tubular central section 2.54 cm in diameter and 50 cm high, and an expansion section at the top. The volume was 700 mL. Air was sparged at the bottom of the bioreactor, through a microporous glass disk covering the whole cross-sectional area, at a flow rate of 15 mL/min. Liquid medium was fed at the bottom of the bioreactor and was continuously measured. Temperature was controlled at 29°C through the reactor water jacket. The pH of the medium was continuously controlled within the 6.4–6.6 range.

Cell aggregates, known as pellets, were used as immobilized cell particles. These were obtained in growth batch cultivations in shaken Erlenmeyer flasks, using an inoculum of spores (5×10^3 spores/mL) in a seed medium containing the following per liter of distilled water: 30 g starch, 2.5 m*M* phosphate (as 7:3 mixture of K_2HPO_4 and KH_2PO_4), 40 m*M* glutamic acid, 0.2 g $MgSO_4 \cdot 7H_2O$, 18 mg $FeSO_4 \cdot 7H_2O$, 1 mg $CaCl_2$, 1 mg NaCl, and 9 mL of trace mineral solution as previously described *(18)*. The medium used for antibiotic production was a modification of this medium using 15 g/L of glycerol as carbon source and 25 m*M* glutamic acid. Phosphate concentration was changed at various points during the experiments ranging from 0 to 0.05 m*M*.

Analysis

Biomass concentration was measured as dry weight at the start point and at the end of the bioprocess. The size of the pellets was measured periodically with a microscope (×40). The average diameter was deter-

mined statistically from samples with a minimum of 30 pellets. The hybrid antibiotic is a pigmented compound, and its concentration was measured as the absorbance at 530 nm at pH 10.0.

Mathematical Model

During the growth phase, mycelial pellets of *S. lividans* are formed under nonlimiting conditions. The process of pellet formation, involving the spore germination and the aggregation of hyphal fragments, is completed within approx 20 h after culture inoculation, and the number of spherical pellets (n_p) does not change after this period. Growth proceeds for 55–70 h more when these pellets exhibit a fairly uniform size, which is dependent on the extension of the growth phase and the culture conditions *(19)*. To bring about the shift from cell growth phase to production phase, the pellets were gently washed and transferred to the fluidized-bed bioreactor with production medium, whose key nutrient was phosphate. Transversal sections of these initial pellets show to be homogeneous (Fig. 1A). Thus, the biomass concentration *(X)* in the bioreactor may be calculated by

$$X = n_p \pi d^3 \rho / (V_R \cdot 6) \quad (1)$$

where d is the initial pellet diameter, ρ is the pellet density, n_p is the number of pellets, and V_R is the bioreactor volume. During the production phase, the bioreactor is fed continuously with medium free of phosphate. In spite of this limitation, the immobilized cells are able to produce antibiotic for a period of 12 d, and the diameter of the pellets slowly increases. A continuing increase in biomass after a phosphate depletion during a batch fermentation has been observed for this type of organism, too *(15,20)*. Under growth conditions with an excess of phosphate, the phosphate can be stored as polyphosphate in amounts of 0.1–20% of dry weight *(21)*. The depletion of phosphate in the medium can result in a shift in the metabolic state from fast to slower growth. The number of pellets remains constant during the entire experiment, as well as the bioreactor volume. Therefore, if the density of the cells is considered constant, the growth of the biomass involves an increase in the diameter. The new biomass concentration *(X)* is related to the initial biomass (X_0) and initial diameter (d_0) as described by Eq. 2:

$$X = X_0 (d / d_0)^3 \quad (2)$$

On the other hand, the initial homogeneity shown in the transversal sections of the early pellets disappears along the culture. Later observations show two main zones: an internal zone, which shows the cell autolysis owing to the lack of nutrients, and an external zone, which is responsible for antibiotic production and the apparent cell growth. Figure 1B shows this differentiation clearly. This differentiation means that an increase in the pellet diameter may not involve a net increase in the biomass concentration.

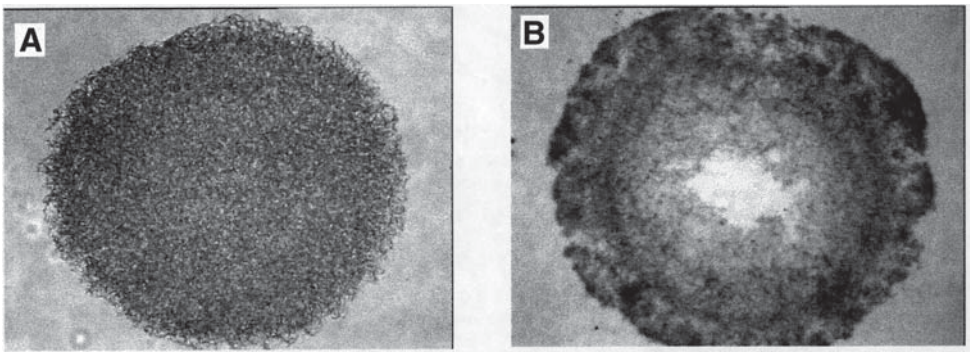

Fig. 1. Microscopic observations of a transversal section of *S. lividans* TK21 pellets immobilized in a fluidized-bed bioreactor **(A)** at the initiation of the operation and **(B)** after 45 d.

The mathematical model developed in this work was based on a number of assumptions. First, the cyclic feeding of phosphate is always maintained at such low levels that the cell metabolism is not shifted to rapid cell growth. Second, antibiotic production is repressed when extracellular phosphate is available. Third, only the cells that have a high level of accumulated intracellular polyphosphate are able to synthesize high levels of antibiotic. The authors postulate these last two points in order to describe the critical role of phosphate. It has not been possible to verify them experimentally owing to the extremely low levels of phosphate used. However, the excellence of the modeled results is a good demonstration of their validity and physical sense. In addition, the long residence time and the internal mixing conditions provided by the fluidization with air bubbles allows the performance of the bioreactor to be considered as that of an ideal continuous stirred-tank reactor.

The model structure is transferred into the state equations for the concentrations of biomass *(X)*, antibiotic *(A)*, and extracellular phosphate *(PE)* in the bioreactor. The internal state variable *(PI)* is represented by the dimensionless level of intracellular phosphate. The cells have been growth in a nonlimited medium, which means that the amount of polyphosphate accumulated is the maximum and that *PI* is assumed to be 1. Consequently, *PI* value will always be between 1 and 0.

The specific growth rate (Eq. 3) consists of two terms:

$$r_X = \mu_X - k_d \tag{3}$$

The first term describes the growth rate of the external zone and the second represents the lysis rate of the internal zone, where k_d is the first-order rate constant for the lysis. The growth rate follows a Monod kinetics up to the depletion of the stored internal phosphate, which is given by Eq. 4. The biomass increase owing to this growth rate involves an increase in the diameter size of the pellet according to Eq. 2.

$$\mu_X = \mu_{max} [PI/(K_X + PI)] \quad (4)$$

where K_X is the coefficient of Monod kinetics.

The balance equation for the immobilized biomass in the bioreactor is therefore given by

$$dX/dt = r_X X \quad (5)$$

The specific production rate is expressed in terms of a Monod kinetics depending on the intracellular phosphate level, modified by a factor that expresses the production inhibition by the presence of extracellular phosphate.

$$r_A = r_{A\,max} [K_a/(K_a + PE)] [PI/(K_{PI} + PI)] \quad (6)$$

The material balance for the antibiotic is given by Eq. 7, where D is the dilution rate in the bioreactor:

$$dA/dt = -DA + r_A X \quad (7)$$

The phosphate is transported into the cell by active transport with a saturation kinetic whose rate is given by

$$r_{PI} = r_{PI\,max} [PE/(K_{PE} + PE)] (1 - PI) \quad (8)$$

The internal phosphate consumption rate is expressed in terms of a constant rate (k_1). The balance of the amount of intracellular phosphate is expressed as follows:

$$dPI/dt = r_{PI} - k_1 - r_X PI \quad (9)$$

The extracellular phosphate is consumed by the biomass owing to the transport into the cell to restore the intracellular phosphate. Therefore, the balance equation is given by

$$dPE/dt = D(PE_f - PE) - Y r_{PI} X \quad (10)$$

where PE_f is the concentration of phosphate in feeding medium and Y has the meaning of yield in the phosphate transport (mmol PO_4^{3-}/g biomass).

Results and Discussion

The model described for the production of a hybrid antibiotic by immobilized cells of *S. lividans* TK21 includes 10 kinetic parameters. Estimation of these parameters is difficult because only two state variables are measured: pellet size (equivalent to cell concentration) and antibiotic concentration. For the examination and identification of the model parameters, two continuous cultivations with different stages (described as 1a, 2a, 2b, and 2c in Table 1) were selected. As a consequence, the kinetic parameters can be independently identified. Detailed examination of the different circumstances occurring in each case is required before proposing a strategy for parameter identification using these data.

Table 1
Summary of Initial Conditions Corresponding to Different Stages of Runs Used for Parameter Identification

Run	Stage	PE (mM)	PE_f (mM)	PI	Period (h)	X_0 (g/L)
1	1a	0.00	0.00	1	292	2.80
2	2a	0.05	0.05	1	170	1.80
	2b	High	0.00	High	384	1.92[a]
	2c	0.00	0.05	Low	478	2.14[a]

[a]Estimated.

The runs selected include several experimental conditions that allow identification of several parameters in each condition instead of performing the evaluation of all the parameters at the same time. For example, during run 1 and stage 1a, the feeding medium does not contain phosphate, which means that there is neither phosphate transport to the cells nor inhibition owing to the presence of extracellular phosphate. Consequently, in such conditions the effect of the decrease in the intracellular phosphate storage level along time can be determined. Conversely, the addition of phosphate in the feeding medium (0.05 mM) in run 2 and stage 2a reflects the effect in the inhibition caused on product formation and also how the intracellular level is maintained high. When the feeding medium is changed to a free phosphate medium, run 2 stage 2b, the inhibitory effect disappears and antibiotic production increases until the intracellular phosphate level becomes too low. At this point (the end of stage 2b) the product formation decreases owing to phosphate depletion. Finally, when phosphate is added to the feeding medium, run 2 stage 2c, the slow increase of the intracellular phosphate level allows the recovery of the metabolic activity and, as a consequence, the antibiotic production. In essence, each phase is dominated by one specific phenomenon, which controls the cell metabolism and therefore the antibiotic production.

One critical aspect in the model development is the phosphate concentration, both intracellular and extracellular, as the cells used in this work have shown a very high sensitivity to very low levels of phosphate. In most of the conditions used, this level is so low that it could not be analytically detected. Therefore, the model itself has been built to provide the estimation of the phosphate concentration.

The pellet morphology used in this work was obtained under nonlimited conditions. As a consequence, it is assumed that at the initial stage of each run (1a, 2a), the intracellular phosphate level is at a maximum level. For the model development, this condition is expressed in terms of a level of the normalized intracellular phosphate equal to 1 (PI = 1). Conversely, the initial extracellular phosphate concentration depends on the medium used to wash the pellets and fill the bioreactor (0 mM for stage 1a and 0.05 mM for 2a). PE_f refers to the phosphate concentration in the feed-

Table 2
Values Obtained for Model Parameters

Parameter	Value
$r_{A\,max}$	2.4 Abs U $[(g/L) \times h]^{-1}$
$r_{PI\,max}$	0.08 h^{-1}
μ_{max}	1.3×10^{-3} h^{-1}
K_a	0.025 m*M*
k_d	7×10^{-4} h^{-1}
K_{PE}	5×10^{-4} m*M*
K_{PI}	250
K_X	0.2
k_1	0.018 h^{-1}
Y	0.08 mmol/g

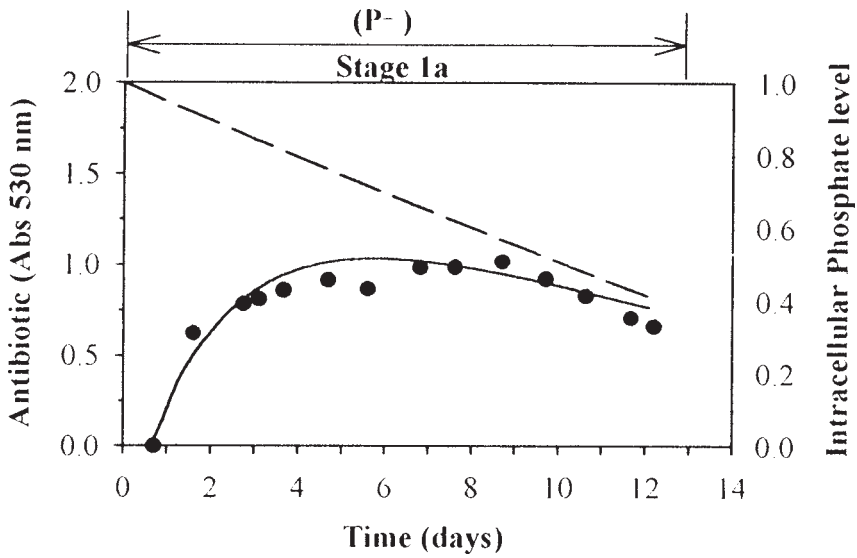

Fig. 2. Experimental antibiotic concentration (symbol), model fit of antibiotic concentration (solid line), and intracellular phosphate level (broken line) corresponding to culture run 1 (stage 1a, Table 1).

ing medium (0 or 0.05 m*M*) depending on the stage. From the second stage until the end of the cultivation, the extracellular phosphate concentration cannot be analyzed owing to its low level, so it will be numerically determined from the mathematical model. After the initial assumption ($PI = 1$), the level of intracellular phosphate will be numerically estimated as well.

The objective function includes the sum of square difference between the simulated state variables and the experimental data. The number of measured points depends on the bioprocess stage. The nonlinear regression problem was solved by the Davison-Fletcher and Powell method *(22)*.

Table 2 summarizes the set of parameters identified by the previously described sequence. Figures 2–5 show the time profiles of the experimental

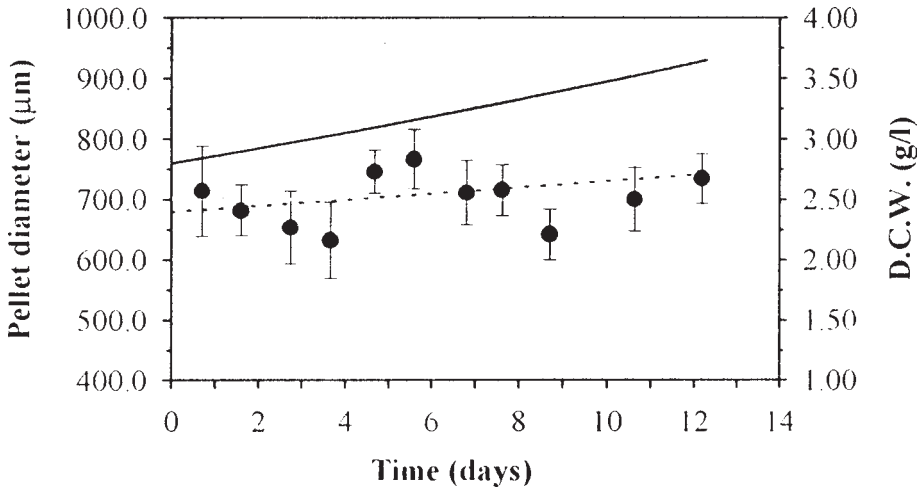

Fig. 3. Experimental diameter of the pellets (symbol), model fit of the diameter (dotted line), and biomass concentration (solid line) corresponding to culture run 1.

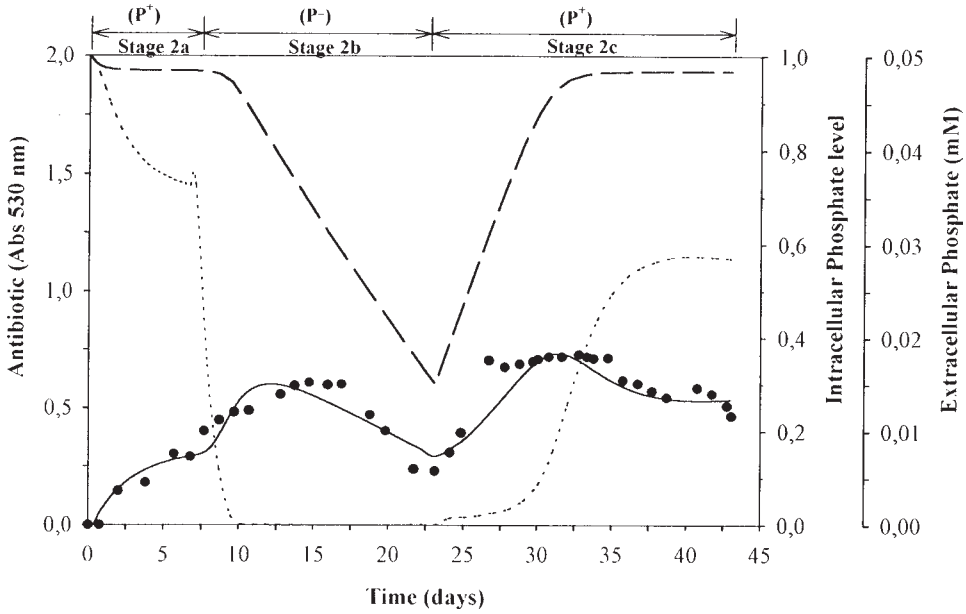

Fig. 4. Experimental antibiotic concentration (symbol), model fit of antibiotic concentration (solid line), intracellular phosphate level (broken line), and extracellular phosphate concentration (dotted line) corresponding to culture run 2 (stages 2a–c, Table 1).

data and model fits, including the concentration of the extracellular phosphate and the intracellular phosphate level estimated by the model.

Using an additional experiment not used previously to determine the parameters of the model has validated the model. This experiment has five

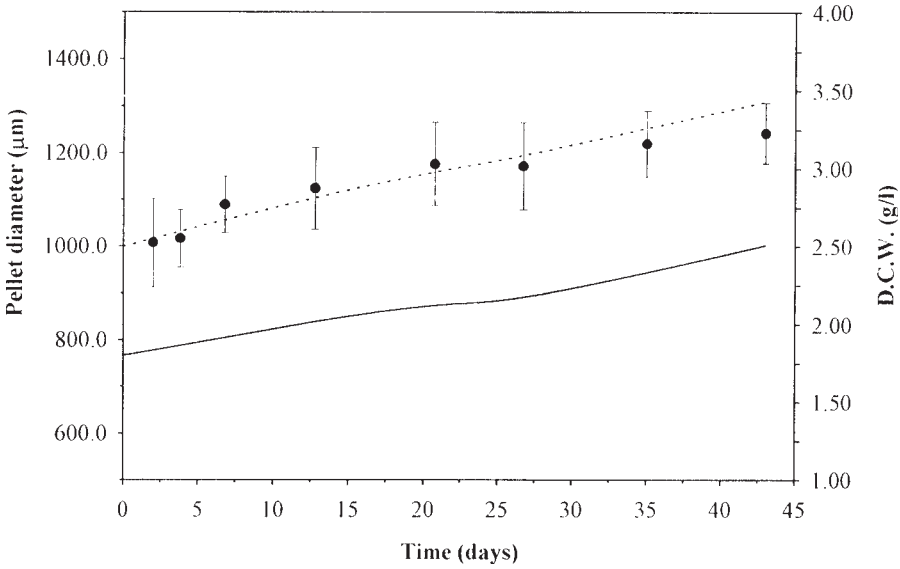

Fig. 5. Experimental diameter of the pellets, model fit of the diameter, and biomass concentration corresponding to culture run 2. Symbols as in Fig. 3.

Table 3
Summary of Initial Conditions Corresponding to Different Stages of Run Used for Model Validation

Run	Stage	PE_0 (mM)	PE_f (mM)	PI_0	Period (h)	X_0 (g/L)
3	3a	0	0.00	1	60[a]	2.00
	3b	0	0.00	High	360	2.05[b]
	3c	0	0.05	Low	192	2.20[b]
	3d	Low	0.00	High	208	2.26[b]
	3e	0	0.05	Low	560	2.35[b]

[a]Batch period.
[b]Estimated.

stages that correspond to different cycles in the bioreactor feeding, performed in order to maintain the antibiotic production for a long period. The strategy for this feeding is to operate at a level of phosphate low enough to trigger antibiotic production, but above the limits leading to the cessation of the metabolic activity. Table 3 summarizes the conditions generated in these five phases of this continuous run 3.

Model simulations are compared with experimental data for the five stages in Figs. 6 and 7 with respect to antibiotic production and pellet size evolution along the culture. It can be seen that agreement is quite good between the experimental data for antibiotic production. However, there appears to be a certain deviation between the measured pellet diameter and the simulation. In spite of this fact, note the good correlation between the

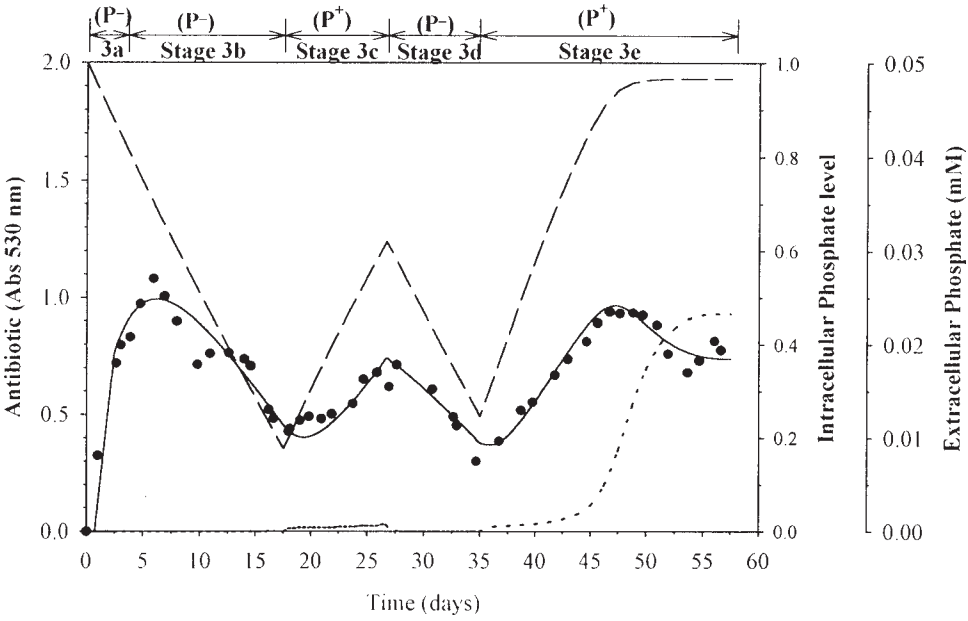

Fig. 6. Comparison of the measured antibiotic concentration and model predictions of antibiotic concentration, intracellular phosphate level, and extracellular phosphate concentration corresponding to run 3 (stages 3a–e, Table 3). Symbols as in Fig. 4.

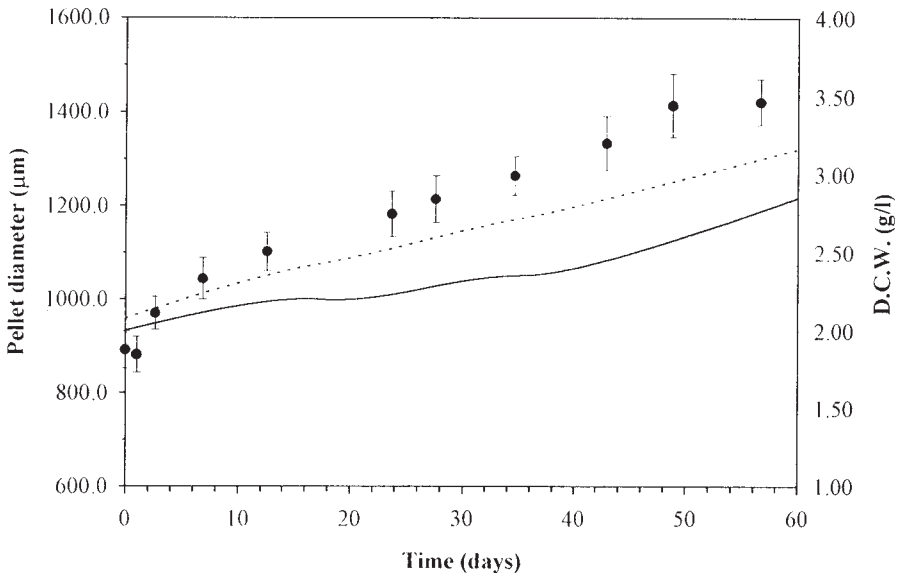

Fig. 7. Comparison of the measured diameter of the pellet and model predictions. Symbols as in Fig. 3.

intracellular phosphate evolution as estimated by the model, and the metabolic activity of the cells, reflected in the antibiotic production. These results corroborate that the continuous production of a hybrid antibiotic

by immobilized cells of *S. lividans* TK21 has a strong dependence on the intracellular phosphate level and the concentration of the phosphate in the medium.

Conclusion

The mathematical model developed in this work allows the satisfactory description of the continuous cultivation experiments in a fluidized bed with *S. lividans* TK21 pellets producing a hybrid antibiotic. The parameters of the model have been calculated in independent sets of experiments, and the model's validity has been further corroborated in the description of a complete bioprocess experiment comprising various cycles with different feed conditions. The obtained results are evidence that the role of the intracellular and extracellular phosphate concentrations is of critical importance in order to build a simple structured model that considers the relationship among phosphate feeding, phosphate storage, and antibiotic production.

Acknowledgment

The authors gratefully acknowledge the financial support of grant BIO89-0243 from the Spanish Comisión Interministerial de Ciencia y Tecnología.

References

1. Vecht-Lifshitz, S. E., Sasson, Y., and Braun, S. (1992), *J. Appl. Bacteriol.* **72,** 195–200.
2. Smith, J., Lilly, M. D., and Fox, R. (1990), *Biotechnol. Bioeng.* **35,** 1011–1023.
3. Megee, R. D., Kinoshita, S., Fredrikson, A. G., and Tsuchiya, H. M. (1970), *Biotechnol. Bioeng.* **12,** 771–801.
4. Matsumura, M., Imanaka, T., Yoshida, T., and Taguchi, H. (1981), *J. Ferm. Tech.* **59,** 115–123.
5. Chu, W. Z. and Constantinides, A. (1988), *Biotechnol. Bioeng.* **32,** 277–288.
6. Nestaas, E. and Wang, D. I. C. (1983), *Biotechnol. Bioeng.* **25,** 781–796.
7. Meyerhoff, J. and Bellgardt, K. H. (1995), *J. Biotechnol.* **38(3),** 201–217.
8. Yang, H., King, R., Reichl, U., and Gilles, E. D. (1992), *Biotechnol. Bioeng.* **39,** 49–58.
9. Nielsen, J. (1993), *Biotechnol. Bioeng.* **41,** 715–727.
10. Nielsen, J. and Krabben, P. (1995), *Biotechnol. Bioeng.* **46(4),** 588–598.
11. Dykstra, K. H., Li, X. M., and Wang, H. Y. (1988), *Biotechnol. Bioeng.* **32,** 356–362.
12. Ross, A. and Schugerl, K. (1988), *Appl. Microbiol. Biotechnol.* **29,** 174–180.
13. Thomas, C. R., Paul, G. C., and Kent, C. A. (1994), *Prog. Biotechnol.* **9(2),** 849–852.
14. Paul, G. C. and Thomas, C. R. (1996), *Biotechnol. Bioeng.* **51,** 558–572.
15. King, R. (1997), *J. Biotechnol.* **52,** 219–234.
16. King, R. and Büdenbender, Ch. (1997), *J. Biotechnol.* **52,** 235–244.
17. Constantinides, A. and Mehta, N. (1991), *Biotechnol. Bioeng.* **37,** 1010–1020.
18. Sarrà, M., Redin, I., Ochin, F., Gòdia, F., and Casas, C. (1993), *Biotechnol. Lett.* **15,** 559–564.
19. Sarrà, M., Casas, C., and Gòdia, F. (1997), *Biotechnol. Bioeng.* **53(6),** 601–610.
20. Mundry, C. and Kuhn, K. P. (1991), *Appl. Microbiol. Biotechnol.* **35,** 306–311.
21. Kulaev, I. S. (1979), *The Biochemistry of Inorganic Polyphosphates*, Wiley, London.
22. Edgar, T. F. and Himmelblau, D. M. (1988), *Optimization of Chemical Processes*, McGraw-Hill, New York.